doi:10.1093/brain/awm324 *Brain* (2008), **131**, 473–484

Is the synchronization between pallidal and muscle activity in primary dystonia due to peripheral afferance or a motor drive?

Andrew Sharott,[1,*] Pascal Grosse,[2,*] Andrea A. Kühn,[2,3] Farid Salih,[2,3] Andreas K. Engel,[1] Andreas Kupsch,[2] Gerd-Helge Schneider,[4] Joachim K. Krauss[5] and Peter Brown[3]

[1]Department of Neurophysiology and Pathophysiology, University Medical Center Hamburg-Eppendorf, 20246 Hamburg, [2]Department of Neurology, Charité Campus Virchow, Humboldt University Berlin, Germany, [3]Sobell Department of Motor Neuroscience and Movement Disorders, Institute of Neurology, London, UK, [4]Department of Neurosurgery, Charité Campus Virchow, Humboldt University Berlin and [5]Department of Neurosurgery, Medical University of Hannover, Germany

*These authors contributed equally to this work.

Correspondence to: Prof. Peter Brown, Sobell Department of Motor Neuroscience and Movement Disorders, Institute of Neurology Queen Square, London WCIN 3BG, UK
E-mail: p.brown@ion.ucl.ac.uk

The pathophysiological mechanisms of primary dystonia have largely remained obscure. Yet there is one undeniable observation: lesioning or high-frequency stimulation of the internal segment of the globus pallidus (GP) ameliorates dystonic symptoms. The latter observation implicates abnormal pallidal activity in the genesis of primary dystonia. Recently, excessive oscillatory pallidal activity in the 3–10 Hz frequency range, synchronized with dystonic EMG, has been related to the occurrence of involuntary muscle activity in these patients. However, it is unclear whether this pathological synchronization is driven by GP, caused by re-afference from dystonic muscle, or due to a combination of these two processes. Here we used the Directed Transfer Function as a spectral measure to identify the degree and direction of coupling across time between GP and muscle in seven patients with primary dystonia. We show that pallidal local field potential activity $\leqslant$ 10 Hz is coherent with dystonic movements, and that although the coupling between GP and activity in the sternocleidomastoid muscle is bidirectional, the drive from GP to muscle significantly outweighs that from muscle to GP. In addition, the net GP drive to muscle is not stable but fluctuates across time, in keeping with the dynamic nature of dystonic muscle activity.

Keywords: dystonia; basal ganglia; electromyography; synchronization; globus pallidus

Abbreviations: GP = globus pallidus; LFP = local field potential; DTF = directed transfer function; FFT = fast Fourier transform; MAR = multiple autoregressive

Received July 4, 2007. Revised December 5, 2007. Accepted December 12, 2007. Advance Access publication January 4, 2008

Introduction

Dystonia is characterized by sustained or intermittent involuntary muscle contractions causing abnormal postures, twisting or repetitive movements. Its pathophysiology has remained unclear. Recent attention has focussed on whether activity in the globus pallidus (GP) could be abnormally patterned in dystonia. In particular, it has become increasingly evident that there is excessive oscillatory activity between 3 and 10 Hz in the local field potential (LFP) of the pallidum in patients with primary dystonia (Liu *et al.*, 2002; Siberstein *et al.*, 2003). This pathological LFP activity reflects the synchronization of local pallidal neurons in this frequency band (Chen *et al.*, 2006*b*) and suggests that the abnormal patterning of discharge of single neurons evident in microelectrode recordings in patients with dystonia (Suarez *et al.*, 1997; Vitek *et al.*, 1999) may be locked across populations of local neurons. Importantly, the pallidal LFP activity in the 3–10 Hz frequency band is correlated and coherent with involuntary dystonic muscle activity (Liu *et al.*, 2006; Chen *et al.*, 2006*a*).

© *The Author (2008). Published by Oxford University Press on behalf of the Guarantors of Brain. All rights reserved. For Permissions, please email: journals.permissions@oxfordjournals.org*

Table 1 Patient's details

Case	Sex	Age (years)	Disease duration (years)	Distribution	Etiology	Pre-op BFM-score[a]	Medication
1[b]	M	42	15	Generalized	Hereditary	37	–
2[b,c]	M	36	29	Generalized	Hereditary	82	Haloperidol Tiaprid Lorazepam
3	F	38	12	Generalized	Idiopathic	16	–
4[b]	F	62	13	Cervical	Idiopathic	34	Propranolol
5[b,c]	M	64	7	Segmental	Idiopathic	23	Diazepam
6[b]	M	74	13	Segmental	Idiopathic	12	Tilidin
7[b,c]	M	40	1	Cervical	Idiopathic	8	Metoprolol Primidone

[a]Burke-Fahn-Marsden rating scale-score-motor. [b]Previously also reported in Chen *et al.*, 2006*b*. [c]Previously also reported in Chen *et al.*, 2006*a*

Critically, however, it is unknown whether the synchronization between pallidal and dystonic muscle activities results from afferent input from muscle to GP, an efferent drive from GP to muscle or a combination of these drives leading to bidirectional flow between GP and muscle. The inferences are very different, and there is evidence to support the existence of both afferent and efferent drives. On the one hand, pallidal neurons may respond to peripheral stimuli and this responsiveness is increased in dystonia (Lenz *et al.*, 1998). On the other hand, spectral analyses of EMG signals from dystonic muscles have identified a pathological descending drive within the 3–10 Hz band with a presumptive, but unproven, origin in the pallidum of patients with primary dystonia (Tijssen *et al.*, 2002; Grosse *et al.*, 2004).

The possibility of bidirectional flow between GP and muscles implies that standard spectral phase estimates of temporal relationships between synchronized pallidal and muscle activities may be unreliable (Cassidy and Brown, 2003). In contrast, another spectral measure, the directed transfer function (DTF), is able to disentangle synchronized oscillations in the presence of bidirectional flow (Kaminski and Blinowska, 1991; Cassidy and Brown, 2003). The DTF is being increasingly used to determine the direction of coupling at different frequencies between different regions of the brain (Korzeniewska *et al.*, 2003; Brovelli *et al.*, 2004; Sharott *et al.*, 2005) and between the brain and muscle (Mima *et al.*, 2001). However, the static DTF ignores the fluctuating character of abnormal muscular contraction, sometimes in the range of seconds, which constitutes one of the clinical hallmarks of dystonia. Thus, the DTF has been adapted to allow the serial analysis of short periods of data in order to capture the temporal dynamics of synchronized oscillations (Sharott *et al.*, 2005).

Here we estimate time-evolving asymmetrical flow in the DTF for short overlapping segments across long recordings of GP and EMG activity, to provide evidence that GP activity on balance drives neck muscles in dystonic patients and, furthermore, that this drive demonstrates the dynamic properties that are at the core of the disorder.

Materials and Methods

Patients and electrode implantation

We examined seven patients (five men, two women; mean age: 51 ± 15 years; range: 36–74) with primary dystonia (idiopathic or hereditary) (Table 1) who underwent bilateral implantation of deep brain electrodes in GPi. In all patients the neck was clinically affected. Disease duration varied between one and 29 years (mean: 13 ± 9 years) and on the Burke–Fahn–Marsden (motor) scale patients scored between 10 and 82 (mean: 31 ± 25). Except for cases one and three, all patients were receiving medication for dystonia.

Patients were recorded 2–6 days post-operatively in the interval between macroelectrode implantation and subsequent connection to a subcutaneously placed stimulating device. The operative procedure and beneficial clinical effects of stimulation have been described elsewhere (Vitek *et al.*, 1998; Volkmann and Benecke, 2002; Krauss *et al.*, 2003). DBS electrodes were inserted bilaterally. The macroelectrode used was model 3387 (Medtronic Neurological Division, Minneapolis, USA) with four platinum–iridium cylindrical surfaces (1.27 mm diameter and 1.5 mm length) and centre to centre separations of 3 mm. Contact 0 and 3 were the lowermost and uppermost contacts, respectively. Macroelectrodes were connected to a battery-operated programmable pulse-generator (Itrel ll or Kinetra 7428, Medtronic) after a post-operative interval of 3–7 days.

Pallidal electrode trajectories were aimed at the postero-ventral portion of the globus pallidus internus (GPi) and the posterior ansa lenticularis. The target was identified on high-resolution T2-weighted axial, coronal and sagittal MRI planes. These images were superimposed on coronal and lateral contrast ventriculography and drawn on the GP Tailairach Scheme, corresponding in location to the GP area in the Schaltenbrand and Wahren atlas (Schaltenbrand and Wahren, 1977). The depth of the lowest contact was aimed to be at least 1 mm above the upper border of the optic tract. The location of the latter was established using the intra-operative induction of visual phosphenes by high-frequency stimulation and/or the measurement of electrical activity from the optic tract. Intra-operative microelectrode recordings and macrostimulation were performed in all patients. The target coordinates for the lower contact were 2–3 mm in front of the mid-commissural point, 20–22 mm lateral to the midline of the third ventricle and 4–6 mm below the anterior commissure (AC)-posterior commissure (PC) line.

Recordings and analysis

Subjects were seated and recorded at rest, simultaneously with spontaneous dystonic posturing or movement of the neck. LFPs were recorded bipolarly from the adjacent four contacts of each pallidal macroelectrode (contacts 01, 12, 23). They were filtered at 0.5–300 Hz. Simultaneous surface EMG recordings were made over the sternocleidomastoid (SCM) bilaterally using pairs of Ag/AgCl electrodes taped 3–4 cm apart over the muscle bellies. EMG was filtered at 16–250 Hz. The high pass band of 16 Hz was chosen so as to limit the effects of movement artefact. Signals were amplified and filtered using a custom-made, 9-V battery-operated portable high-impedance amplifier (which had as its front end input stage the INA 128 instrumentation amplifier, Texas instruments, Dallas, TX, USA) and sampled at 625–1250 Hz through a 1401 analogue to digital converter (Cambridge Electronic Design, Cambridge, UK) onto a portable computer using Spike2 software (Cambridge Electronic Design).

Data analysis

All analysis was conducted on one long data segment lasting between 140 and 200 s (mean: 191 ± 22.6 s) recorded for each patient. To maximize the amount of data used, the whole record was used in each case and *post hoc* statistical measures used to normalize for differences in data duration (see later). EMG signals were DC corrected and rectified before spectral analysis. All analyses were performed in MATLAB (Mathworks Inc., Massachusetts, USA).

FFT analysis

To establish consistency with previous studies, EMG and GP-LFPs were first analysed in the frequency domain by calculating Fast Fourier Transform (FFT)-based power and coherence spectra using 1 Hz frequency resolution. Note that neither this approach, nor the DTF employed in the main analysis, adequately characterize non-oscillatory synchrony, which was therefore not the object of this study. Power was expressed as percentage of total power over 2–40 Hz to normalize the data across patients. Power at very low frequencies (<2 Hz) was excluded so as to minimize the contribution of movement, respiration and pulse artefact and 'DC drift'. The low 40 Hz cut-off removed any risk of contamination by mains artefact. These percentage power values were averaged across LFPs from different contacts and EMGs from the two muscles for statistical analysis. As the length of the recordings used was variable and the confidence limit is dependant on the total number of FFT windows, a confidence limit (95%) was calculated for each record as described in Halliday *et al.* (1995). Coherence values were then Fisher transformed prior to any averaging. In each frequency bin, the number of significant bins was then counted across GP-LFP/SCM-EMG combinations in each patient (any one combination from each patient could therefore only contribute one significant bin at any frequency), summed and then normalized to give the percentage of significant bins at each frequency. The absolute value of the imaginary coherence, the imaginary part of the standard coherence calculation, was used as a measure of phase locking without synchronization at zero phase (Nolte *et al.*, 2004) and was also Fisher transformed.

Directed transfer function analysis

A detailed description of the methodology and principles of the DTF can be found in Kaminski and Blinowska (1991), Korzeniewska *et al.* (2003) and Cassidy and Brown (2003). The DTF technique relies on the key concept of Granger causality between time series (Granger, 1969), according to which an observed time series $x(n)$ causes another series $y(n)$ if the knowledge of $x(n)$' s past significantly improves prediction of $y(n)$. The latter relationship between time series is not reciprocal, i.e. $x(n)$ may cause $y(n)$ without $y(n)$ necessarily causing $x(n)$. This lack of reciprocity enables the evaluation of the direction of information flow between structures. To this end, the multiple autoregressive (MAR) model that best described the signals coming from the two regions of interest is determined. The MAR methodology is essential for the DTF, as the DTF is built directly from the MAR coefficients. Following the procedure detailed in Cassidy and Brown (2002), a Bayesian methodology was applied to estimate the parameters of the autoregressive model. This approach is desirable in that it provides full probabilistic distributions for all of the model parameters. The autoregressive coefficients can be used to construct a bounded, normalized measure (the DTF) that provides information on the effective direction of coupling.

Two possible methodological limitations of the bivariate DTF approach used here should be considered further. First, a general concern in all DTF analyses is whether spurious asymmetries of information flow can be generated through a poor signal to noise ratio (SNR) in one or more of the signals under consideration. This issue has been evaluated with respect to EEG where it has been noted that estimates are reasonable provided SNRs $\geqslant 3$ and $\geqslant 4800$ data samples are available (Astolfi *et al.*, 2005). Our data sets far exceeded this sample limit and the SNR of LFP signals likely exceeds that of EEG (Regan, 1989). The SNR of EMG with respect to descending drives is more difficult to estimate, but it is noteworthy that the power over 3–10 Hz is a major component of EMG in dystonia (see 'Results' section) and this was our band of interest in the current study. Nevertheless, the morphology of EMG motor unit spikes should be considered as a source of non-stationary noise. We tackled this by demodulating the EMG through rectification and low pass filtering at 40 Hz. However, more sophisticated pre-processing approaches have also been used prior to coherence estimations (Wang *et al.*, 2004, 2007).

Second, some methodological and experimental studies advocate the use of multivariate analysis (Korzeniewska *et al.*, 2003; Supp *et al.*, 2005) and even suggest bivariate analysis may lead to spurious results (Kus *et al.*, 2004). However, the potential advantages of the multivariate model can only be fully realized if all strategically important nodes in a circuit can be recorded, which is seldom the case in human studies (see 'Discussion' section). In the case of evaluating information flow between deep brain LFPs and EMG, we do not feel that multivariate analysis confers a clear advantage. In this regard, bivariate analysis has been successfully deployed in a similar context, the investigation of cortico-muscular relationships (Mima *et al.*, 2001). In addition, the interpretation of the bivariate DTF is fairly straightforward (Sharott *et al.*, 2005) and is discussed further below. For such bivariate analysis, at any given frequency, this consists of two directed coherence values giving the coherence in each direction, here either GP-SCM or SCM-GP. If the directed coherence is significantly greater in one direction, the DTF can be

considered 'asymmetric' in that direction. Conversely if the directed coherence estimates are not significantly different the DTF can be considered 'symmetric' (Sharott *et al.*, 2005). Statistical evaluation of these relationships is discussed later.

For each subject, data were organized so as to consist of separate pairs consisting of one GP-LFP and SCM-EMG signal. For each subject six LFP (three bipolar derivations from each hemisphere) recordings and two SCM-EMG (one from each side) were paired, leading to 12 bivariate analyses for each subject. To better model the frequencies of interest, data segments were down-sampled to 80 Hz (after appropriate low-pass filtering to avoid aliasing).

Time/frequency DTF

Time/frequency DTF analysis was used to investigate whether the effective direction of coupling between pallidum and muscle was stationary or dynamic. This involved calculating the DTF for short segments (2–10 s) across the record. For visualization purposes we used the 'net DTF', a mixed product of the asymmetry and the strength of correlation. In deriving this, the coherence values in one direction in each window (e.g. effective direction of coupling from SCM to GP) were made negative and summed with those positive values in the opposite direction. This gave a single value (net DTF) in each frequency bin, with the direction of asymmetry, if present, represented by the sign (e.g. negative when effective direction of coupling is from muscle to GP, and positive when effective direction of coupling is from GP to muscle), and the magnitude of that asymmetry represented by the coherence value. For example a value of +1.0 would represent: (i) all activity in that frequency bin being completely coherent and (ii) coherent activity being completely asymmetric and all coupling in the direction of GP to EMG (Sharott *et al.*, 2005).

For the main group analysis, plots were constructed using DTF coherence values calculated in consecutive 10 s windows with 5 s overlap. Group time/frequency DTFs were examined in two ways. First, the DTF values for each bin across time were averaged. Secondly, the number of significant bins in each direction was summed and normalized over time bins for each frequency bin (resolution 0.4 Hz). These values were averaged across all GP-LFPS/SCM-EMG pairings to give values for bins with DTF values directed from GP-SCM and bins with DTF values directed from SCM-GP. Shorter windows (the lowest being 2 s) were also used for some analyses to verify that the results were not dependant on the time window used. For single examples of time/frequency DTF, spectra were calculated in 15 s windows with a 14 s overlap, to give a smoother time/frequency plot (Fig. 3).

However, DTF values in a given direction do not necessarily mean that DTF values represent a significant asymmetry in that direction at a given time and frequency. To evaluate this, we utilized the confidence limits (set here at 99%) calculated for each individual DTF plot (Cassidy and Brown, 2003). At any given time/frequency point, values were only considered significant if the confidence limits for one or both directions did not take in zero. In addition, values were only considered significant if the lower confidence limit of the greater value was greater than the upper confidence limit of the smaller value (essentially the lower and upper confidence limits of upper and lower traces should not cross). All values that violated these criteria were set to zero. Where as previously, significance was assessed across subjects (Sharott *et al.*, 2005), this method allowed us to attribute significance to a short window of data. In addition, we excluded all activity with symmetrical coherence, which could therefore not be unequivocally attributed to afferent or efferent processes. Symmetrical coherence itself might represent common movement artefact in both channels (most likely due to movement of leads with involuntary head movement) or zero-phase steady-state oscillatory activity between GP and muscle (unlikely given the long conduction delays involved).

Statistics

The 3–10 Hz band has already been identified as characteristic of dystonic brain and muscle activity (see 'Introduction' section). After confirmation that this was the case in the data presented here (Fig. 1), this band was compared with three 'control' bands with the same number of frequency bins outside of the 3–10 Hz range: 15–22, 23–30 and 33–40 Hz. It should be stressed that the final evaluation of activities across bands represents a practical alternative to the comparison of activities at individual frequencies which helps limit the problem of multiple comparisons entailed with the latter approach. Nevertheless, it is possible that our 3–10 Hz frequency band of interest contained both base frequencies and harmonics of dystonic tremor. This in itself should not represent a problem, but confounds could potentially arise if harmonics extended into other 'control' bands of higher frequency. The latter would lead to an underestimation of the physiological significance of spectral differences.

For the analysis of large records (non-time resolved), statistical analysis of spectral parameters was carried out in two ways. First, when the raw spectral measures were considered, i.e. power/transformed coherence values in bands of interest, Kruskal Wallis tests were used to establish whether there were differences across frequency bands for grand averages of muscle, pallidal and muscle/pallidal pairs across patients. *Post hoc* Wilcoxon Sign Rank tests were then used to specifically test whether spectral measures were significantly different between the 3–10 Hz band and the test bands. Significance for multiple comparisons was corrected using the step down procedure. In the case of the DTF, Friedman tests were used to perform a two-way analysis of variance incorporating both frequency band and direction. Multiple comparison corrected Wilcoxon tests were then used to compare the DTF in each direction across frequency bands and DTF in the two directions in the dystonic band. Secondly, where significant bins were counted across all subjects, conditions (bands, directions, laterality) were compared using either Fisher's exact or Wilcoxon Sign Rank tests as appropriate.

Focality in the DTF results was examined by calculating the total number of significant bins at each of the three contact pairs in each electrode ($n = 14$) for all frequency bins in the 3–10 Hz range. These values were tested against the null hypothesis that the total number of significant bins for each electrode is evenly distributed across the three contact pairs, using the Chi-squared test (Preacher, 2001). Using this method it was possible to evaluate focality in each electrode individually.

Results

FFT power and coherence analysis

Peaks were observed at 3–10 Hz in the power spectra of GP and SCM activity in both individual contact-muscle pairs and in the group average (Fig. 1A–C). There was a

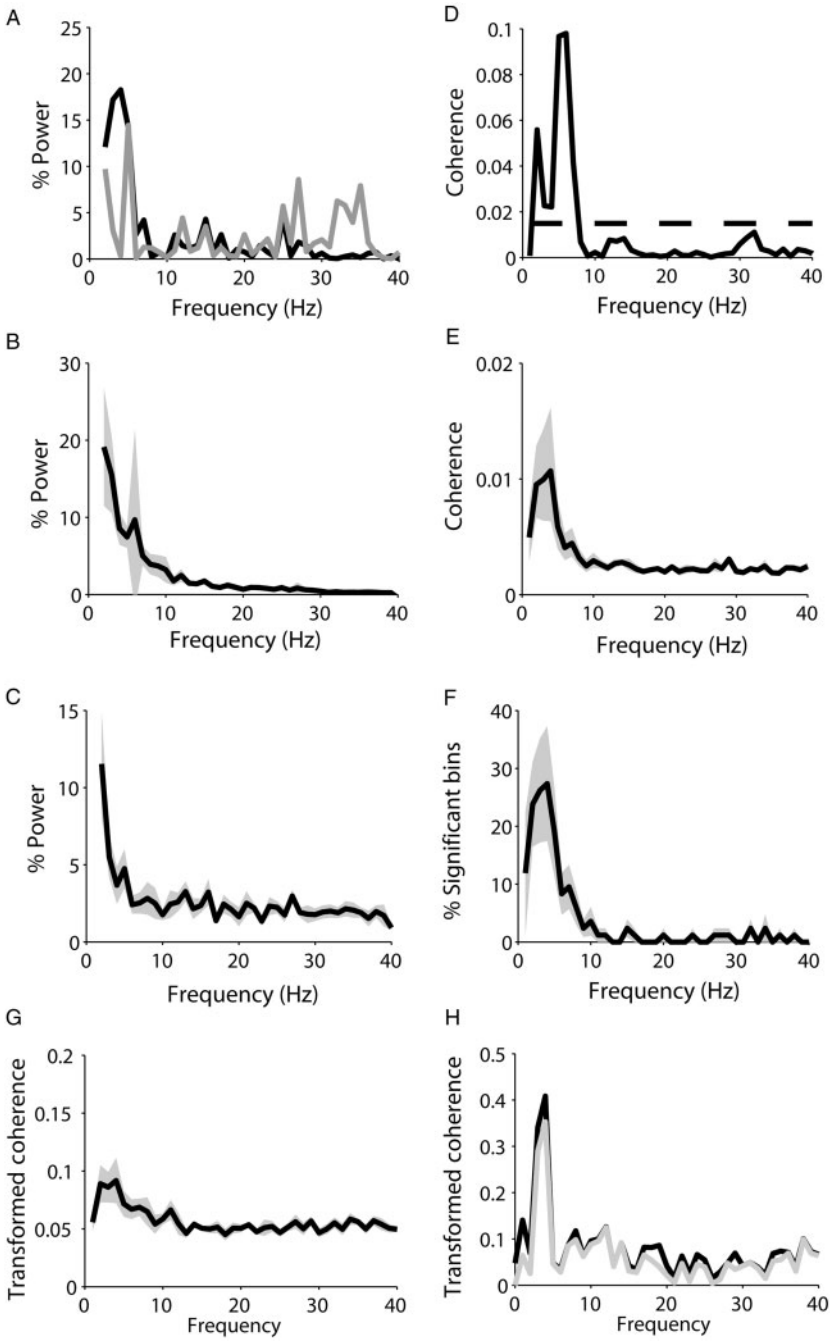

Fig. 1 FFT-based analysis of GP-LFPs and EMG from dystonic patients. (**A**) Power spectra for one bipolar GP-LFP (black line) and ipsilateral SCM-EMG (grey line). Both display a prominent power in the 3–10 Hz range. (**B** and **C**) Group mean power spectra for all GP-LFPs and SCM-EMGs, respectively. Both display peaks in the 3–10 Hz range. (**D**) Coherence spectrum between the GP-LFP and EMG in A. Coherence is most prominent in the 3–10 Hz range where there is a broad, significant peak (95% confidence limit is shown by the dotted line). (**E**) Group mean coherence for all GP-LFP/SCM-EMG pairs. Coherence is elevated in the 3–10 Hz band. The confidence limit is not shown due to the different record lengths used. (**F**) Significance was established by counting the percentage of significant bins at each frequency for all GP-LFP/SCM-EMG pairs in each subject. The plot shows a clear peak in the 3–10 Hz range. (Grey shaded areas represent ± SEM across subjects). (**G**) The equivalent average of the absolute value of the imaginary part of the coherence also has a peak at 3–10 Hz. (**H**) A plot of coherence (black) and imaginary coherence (grey) in one GP-SCM pair.

significant difference in the power between the four frequency bands (dystonic 3–10 Hz and three test bands spanning 15–22, 23–30 and 33–40 Hz) for both SCM (Kruskal Wallis Test, $P = 0.005$) and GP (Kruskal Wallis Test, $P = 0.00005$). For SCM, power in the 3–10 Hz band was significantly higher than in all the control bands (Wilcoxon Sign Rank Test, $P < 0.05/0.016/0.016$ for test bands in ascending order of frequency). Similarly, peaks in the coherence were observed at

frequencies ⩽10 Hz that were often highly significant for individual contact-muscle pairs (Fig. 1D). A significant difference was found in mean Fisher transformed coherence between the four frequency bands (dystonic 3–10 Hz and three test bands, Kruskal Wallis Test, $P = 0.01$). Coherence at 3–10 Hz was significantly greater than in all control bands (Wilcoxon Sign Rank Test, $P < 0.016/0.03/0.016$ for test bands in ascending order; see Fig. 1E). A similar result was found using the mean percentage significant bins in each frequency band (dystonic 3–10 Hz and three test bands, Kruskal Wallis Test, $P < 0.01$, see Fig. 1F), with more significant bins in the 3–10 Hz band than all test bands (Wilcoxon Sign Rank Test, $P = 0.03$, all bands, see Fig. 1F). As in previous studies (Silberstein *et al.*, 2003; Lui *et al.*, 2006; Chen *et al.*, 2006*a*), oscillations at low frequency therefore appeared to be a marked feature in the pallidal LFP and muscle of dystonic patients.

In addition to power and coherence, the imaginary coherence was computed. Whereas the value of coherence is dependant on phase and power, the imaginary coherence uses only the imaginary component of the complex number. This has two benefits, firstly a high value is dependant on phase locking between channels and secondly, it is not influenced by phase locking between the signals at zero phase (Nolte *et al.*, 2004). As the imaginary coherence can be positive or negative depending on the phase delay between signals, the absolute value was taken (and Fisher transformed as with coherence). The mean imaginary coherence showed a similar increase to the standard coherence over 3–10 Hz (Fig. 1G and H). This suggests that at least some of the coherence between GP and dystonic muscle is dependent on phase locking alone (and independent of amplitude correlation between the two signals) and that this is also not due to common artefact such as cable movement. When considered together with the predominant DTF from GP to muscle (see later), the implication is that the phase of pallidal oscillatory activity in the 3–10 Hz band helps dictate the phase of the dystonic EMG activity, pointing to a direct relationship between the two.

Static DTF analysis

To examine the directional relationships for coherent activity between pallidum and muscle, DTF analysis was first performed on the long data records described earlier. Friedman tests of the mean Fisher transformed DTF with respect to direction (GP to SCM and SCM to GP) and frequency band (four levels as above) showed significant effects for both parameters ($P < 0.005$ and $P < 0.01$, respectively). *Post hoc* tests showed that DTF was higher from GP-SCM than vice versa in all bands (Wilcoxon Sign Rank Test, $P < 0.016$) and that DTF was higher in the 3–10 Hz range than all test bands in both directions (Wilcoxon Sign Rank Test, GP-SCM: $P < 0.016$, SCM-GP: $P < 0.016/0.016/0.05$ in ascending order of frequency; see also Fig. 2A). As DTF analysis applied to non-linear data is sensitive to sampling step size, the raw DTF was calculated over a range of sampling rates/frequency resolutions from 50 to 90 Hz. This made little difference to the results.

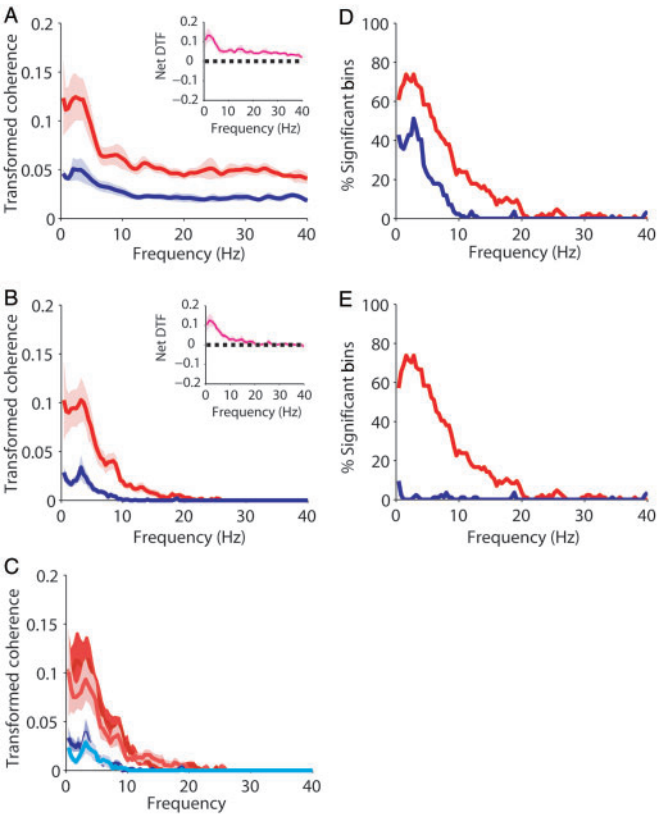

Fig. 2 Directional analysis of GP-SCM coupling. (**A**) Group mean DTF for all GP-LFP/SCM-EMG pairs. DTF from GP to SCM is shown in red, and that from SCM to GP is in blue. DTF from GP to SCM was greater across all frequencies as reflected by the net DTF, which was positive at all frequencies (purple, inset). (**B**) Group mean DTF as in A, but with all non-significant bins (as defined by the confidence limits taking in zero or crossing between the two directions) set to zero. The asymmetry is now specific to lower frequencies as reflected by the net DTF (inset). In both plots, lighter shaded areas represent plus/minus SEM across subjects. (**C**) The corrected DTF (as in B) shows little difference when split in to ipsilateral (dark red/blue) and contralateral (lighter red/blue) pairings. (**D**) Percentage significant bins at each frequency across all patients, contacts and muscles for DTF from GP-SCM (red) and SCM-GP (blue). Despite the relatively low DTF estimates in the 3–10 Hz band in B, 15–60% of these estimates were significant, with a higher amount for GP to SCM. (**E**) Plotting all significant bins as a function of whether they have a net positive (red) or negative (blue) DTF, however, shows that nearly all bins have a higher DTF from GP to SCM, even when the DTF in both directions was significant.

Following removal of all DTF values which were not significantly different from zero or where the information flows in each direction were not significantly different (Fig. 2C), there were still significant effects for both direction (Friedman Test, $P = 0.0002$) and frequency band (Friedman Test, $P < 0.00000001$). In *post hoc* tests, however, direction was only significantly different in the 3–10 Hz

band, with a larger DTF from GP-SCM than vice versa (Wilcoxon Sign Rank Test, $P<0.016$). The DTF was greater in both directions in the 3–10 Hz band than in all test bands (Wilcoxon Sign Rank Test, $P<0.016$), where the DTF was negligible (Fig. 2B). Separating these results in to ipsilateral and contralateral GP-SCM pairs did not significantly alter the results (Fig. 2C).

This observation was extended by examining the incidence of significant bins (as defined earlier) for each direction irrespective of the magnitude of the DTF and which direction was greater. In this case, the number of significant bins for each frequency (resolution 0.4 Hz) was summed across all records (7 patients × 6 GP × 2 SCM = 84). These results, illustrated in Fig. 2D (as a percentage), show that there were many more significant bins in the DTF of both directions in the 3–10 Hz band than at other frequencies. To confirm this, the numbers of significant and non-significant bins were averaged separately across the 3–10 Hz band and compared to the same measures for the 15–22 Hz band (given the obvious decrease with frequency, see Fig. 2D, the other bands were not tested in this case). There were more significant bins in the 3–10 Hz band in both directions (Fisher exact test, GP-SCM: $P<0.000001$, SCM-GP $P<0.00002$). In addition, within the 3–10 Hz band there were more significant bins from GP-SCM than from SCM-GP (Fisher exact test, $P<0.00005$), suggesting that although there is 3–10 Hz activity in both directions, a greater amount of it was in the direction of brain to muscle. To extend this observation further, the number of significant bins was counted in relation to whether they had a positive or negative net DTF (a positive DTF indicating that for a pair of significant values, coherence was greater in the direction GP to SCM than vice versa as in Fig. 3A and B). This revealed significantly more bins with a positive net DTF (red line, Fig. 2E) and negligible bins with a negative net DTF in the 3–10 Hz band (Fisher exact test, significant positive versus significant negative bins, $P<0.00000001$). Together, these results suggest that information flow between pallidum and muscle in the 3–10 Hz band occurs in both directions, but is significantly asymmetric with more information flow directed from brain to muscle.

Time evolving DTF analysis

DTF analysis of long data segments provides an overall picture of the symmetry of directed activities between pallidum and muscle, but does not reveal the true temporal dynamics of this relationship and its consistency for a given GP-SCM pair over time. Accordingly, we performed the DTF on short data segments across records to investigate the temporal consistency of the relationship between the LFP and EMG. Figure 3A and B shows the time-evolving DTF between pallidum and both SCM muscles corresponding to the time-evolving pallidal power spectrum in Fig. 3C. There is a preferential drive from the right pallidum to either SCM at around 4 Hz, but importantly this drive is

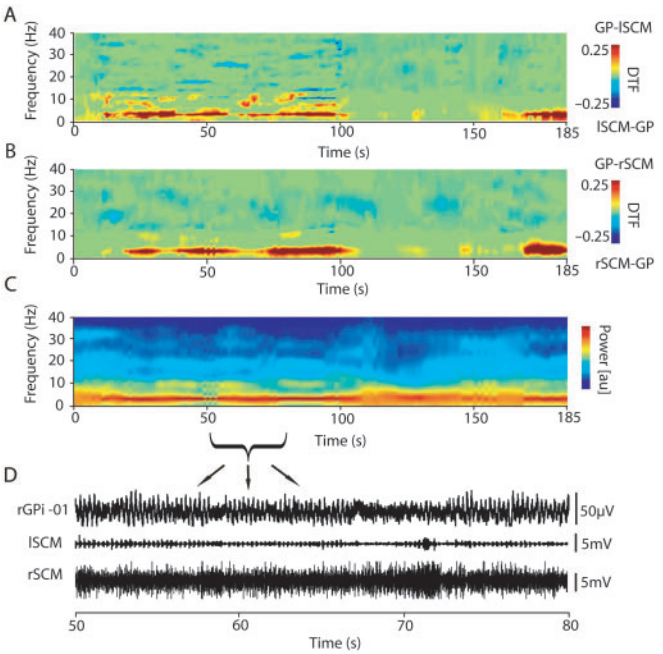

Fig. 3 Single example of coincident dynamics in dystonic EMG activity and pallidal-muscle coupling. (**A** and **B**) Time frequency DTF plots for RGP-RSCM and RGP-LSCM. There is preferential information flow from right pallidum to either SCM at around 4 Hz, but this is dynamic. (**C**) Time–frequency plots of pallidal power over the whole recording. (**D**) Section of raw EMG and pallidal LFP. Oscillatory activity at about 4 Hz is evident for most, but not all, of the record in both LFP and EMG from left SCM.

dynamic, coming and going over time in step with changes in pallidal power at similar frequencies.

To analyse these features across the whole group we first investigated whether the results taken from small data segments broadly matched those achieved using whole recordings. To this end, the time-evolving DTF was averaged across all blocks of time, before being averaged across contacts/muscles as described in the previous section. A Friedman test demonstrated a significant effect for direction, which was larger in the direction of GP-SCM, irrespective of frequency band (Friedman Test, $P<0.000000001$, Wilcoxon Sign Rank test, all bands: $P<0.016$ and see Fig. 4A). When only bins with values significantly different to zero were considered (rather than all bins), there was still a significant effect for direction (Friedman Test, $P<0.001$) and the DTF for GP-SCM was still significantly greater than the DTF for SCM-GP, although only in the 3–10 Hz band (Wilcoxon Sign Rank test, $P<0.016$ and see Fig. 4B). In addition, for both raw and significance corrected DTFs, there was a significant effect for frequency (Friedman Test, $P<0.000001$), with the 3–10 Hz activity greater than all test bands in both directions (Wilcoxon Sign Rank test, $P<0.016$). These results were consistent irrespective of the time bins used (Fig. 4C) and were therefore unlikely to be a result of the time range chosen. When records were tested individually

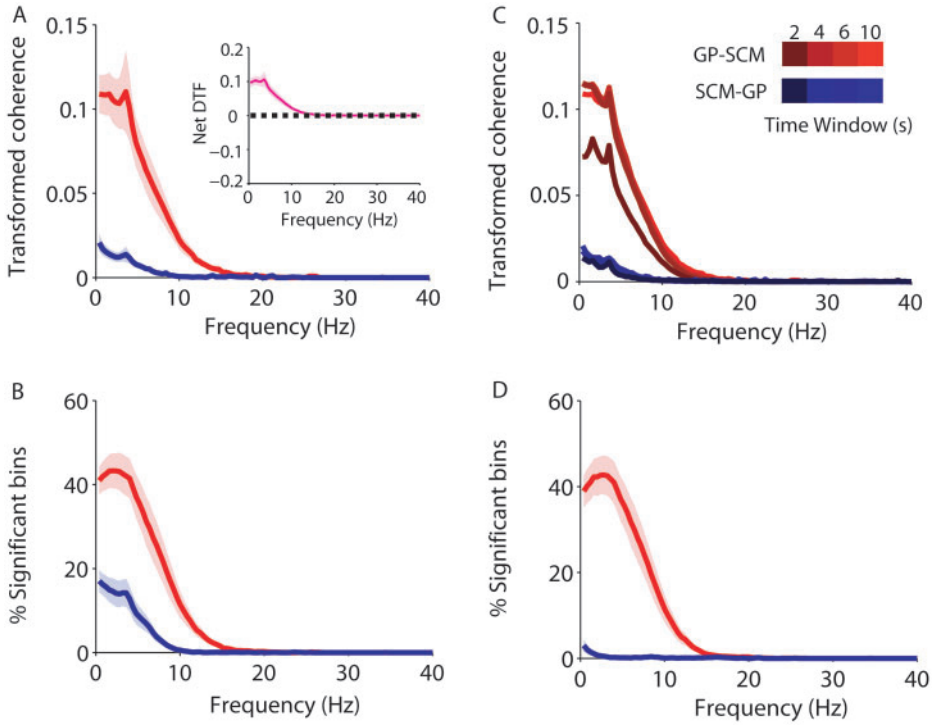

Fig. 4 Statistical evaluation of dynamic coupling of pallidum and muscle. (**A**) Across the group, mean DTF confirmed significant information flow in both directions that was bigger from GP to SCM. (**B**) Corresponding DTF histograms limited to bins with values significantly different to zero concur with this result. (**C**) Mean DTF plots (as in A) for four different time windows between 10 and 2 s. The asymmetry persists with respect to GP-SCM (red hues) and SCM-GP (blue hues) (**D**) Group histogram of% of bins that were both significantly different to zero and were significantly asymmetric shows that even in the 10 s time window, information flow was nearly always bigger from brain to muscle.

for time-evolving differences between directions, 84% had a significantly larger DTF from GP-SCM than SCM-GP in the 3–10 Hz band across time (Wilcoxon Sign Rank test, $P < 0.0042$).

The results were mirrored by those calculated using bins that displayed values that were both significantly different to zero and were significantly asymmetric (data exceeding both significance criteria scored as 1; see 'Methods' section), and counted across time windows for each record. Across subjects there was a significant effect for frequency (Friedman Test, $P < 0.00000001$), with the 3–10 Hz activity significantly greater than all test bands in both directions (Wilcoxon Sign Rank test, $P < 0.016$). There was also a significant effect for direction (Friedman Test, $P = 0.0002$), with the number of bins greater from GP-SCM more than the number of bins greater from SCM-GP in the 3–10 Hz band (Wilcoxon Sign Rank test, $P < 0.016$). Analysis of individual records showed that 67% (Fisher Exact Test, $P < 0.05$) had more significant bins in the direction of GP-SCM than SCM-GP. In the 3–10 Hz range, each record had $29 \pm 2.0\%$ significant bins in the direction GP-SCM. For SCM-GP, the average percentage of significant bins per record was $6 \pm 0.6\%$, suggesting that muscle to brain activity was a relatively more sporadic feature over time. As for the static DTF analysis, when the numbers of significant bins in the 3–10 Hz range were counted in relation to whether they had a positive or negative net DTF, virtually all bins were asymmetric in the direction of GP-SCM (Wilcoxon Sign Rank test, $P < 0.016$ and see Fig. 4D).

Focality of time/frequency DTF analysis

It is not possible to know the exact location of the recording contacts with current imaging methods. However, if the activity described above was focal (to the pallidum or even specific parts of the pallidum) it should be unevenly distributed across the three bipolar derivations. To this end, we compared the total number of significant bins found at each contact with the number of significant bins expected by chance (total significant bins divided by three) in all frequency bins in the 3–10 Hz range averaged over the two muscles. Each pallidal electrode was tested individually (7 patients × 2 hemispheres) for both directions. For the GP-SCM DTF, 11/14 electrodes had significantly uneven distributions of significant bins (Chi-squared Test, $P < 0.0005$). For SCM-GP DTF, 8/14 electrodes had significantly uneven distributions (Chi-squared Test, $P < 0.02$). Given the extremely low number of significant features outside of the 3–10 Hz band, this analysis was not performed on the test bands. There was no evidence that

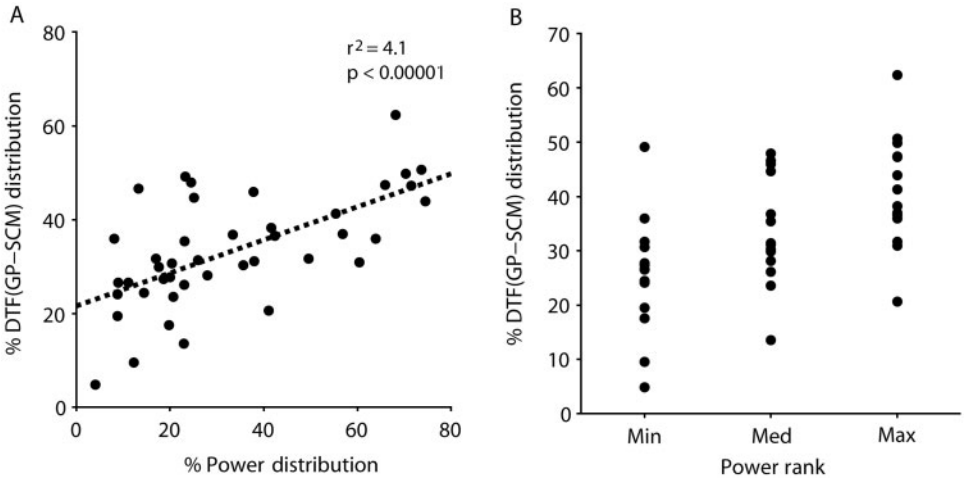

Fig. 5 GP contact pairs with highest power correlate with those with the most consistent GP-SCM DTF. (**A**) Correlation between the distribution of the total number of significant bins for the GP to SCM DTF (meaned across both SCMs) with the corresponding distribution of power in the 3–10 Hz range for all six contact pairs (two sides in each patient). (**B**) The number of significant bins plotted against the contacts arranged according to power (from minimum to maximum on each side).

this focality was more prevalent in contralateral or ipsilateral pairings.

To provide further evidence of focality of the drive from pallidum to muscle we determined whether the bipolar contact pair in GP with the highest power also had the highest number of significant bins in the DTF from GP to SCM. This was examined in two ways in the 14 hemispheres each with 3 bipolar derivations. First, the distribution of the total number of significant bins for the GP to SCM DTF (meaned across both SCMs) was correlated with the corresponding distribution of power in the 3–10 Hz range for all six contact pairs (two sides in each patient). A highly significant positive correlation ($r^2 = 0.41$, $P < 0.00001$) was found, suggesting that the distribution of pallidal power and GP to SCM DTF tended to correspond (Fig. 5). Secondly, each triplet of GP contact pairs was examined individually. In 8/14 hemispheres the position with the highest power exactly matched the position with the highest number of significant bins in the GP to SCM DTF. In addition, when the number of significant bins was plotted against the contacts arranged according to power (from minimum to maximum on each side), there was a clear trend towards the contact with the highest power having the most consistent GP to SCM DTF.

Discussion

We have confirmed that in patients with primary dystonia, pallidal and dystonic muscle activities are coherent over a frequency band of 3–10 Hz (Liu *et al.*, 2006). Furthermore, we have shown that the flow of information between muscle and pallidum is bidirectional, but with significantly more information flow passing from pallidum to muscle in this frequency band. The latter favours a causal link between synchronisation of pallidal activity $\leqslant$10 Hz and dystonic muscle activity. The DTF analysis used here represents a significant advance over previous analyses. These have either ignored the directionality of coupling (Liu *et al.*, 2006; Chen *et al.*, 2006*a*) or, in the one patient where analysis was possible, deduced directionality from phase differences (Foncke *et al.*, 2007*a*), an approach that may be flawed in systems with bidirectional connectivity (Cassidy and Brown, 2003). Moreover, the time/frequency DTF analysis presented here clearly shows that the information flow from pallidum to muscle at 3–10 Hz is not stable but fluctuates across time, in keeping with the dynamic nature of dystonic muscle activity, -something that could not be concluded from previous approaches (Liu *et al.*, 2006; Chen *et al.*, 2006*a*; Foncke *et al.*, 2007*a*).

The DTF has two potential advantages over spectral phase estimates. First, it does not assume unidirectional flow—an assumption that can potentially lead to erroneous physiological conclusions (Cassidy and Brown, 2003). On the other hand the DTF is relatively insensitive when phase/temporal differences between signals are small (Cassidy and Brown, 2003). There is no reason to think this is the case in the coupling between pallidal LFP and muscle, given the indirect connectivity. Second, the estimation of temporal differences from phase spectra is best performed through linear regression analysis of phase over periods of significant coherence (Mima and Hallett, 1999; Grosse *et al.*, 2002). This, in turn, requires peaks in coherence that are reasonably broad, to allow for several phase estimates. This is not always the case in analyses of the relationship between pallidal LFPs and dystonic EMG (Foncke *et al.*, 2007*a*, *b*).

Coupling or coherence implies functional connectivity (Thatcher *et al.*, 1986; Rappelsberger and Petsche, 1988; Nunez, 1995; Shen *et al.*, 1999; Buzsáki and Draguhn, 2004; Magill *et al.*, 2006). Both simple coherence and DTF were consistent with functional connectivity between pallidum and muscle under dystonic conditions. The DTF was often

bidirectional, but where functional connectivity involved coupling directed predominantly from one source, as indicated by an asymmetric DTF, this source can be considered the driver, provided there is biological evidence to support such a causal connection and to refute the possibility of a common input to both signals (Sharott *et al.*, 2005). In the latter case, for example, oscillations could propagate from cortex to both pallidum and muscle, but reach pallidum first, leading to the appearance of a pallidal drive to muscle. With these important provisos, however, there are reasonable examples of interpretable coupling. A ready example that has received much interest of late is corticomuscular coherence in which cortical activity precedes coupled muscle activity, and is equated with a drive from cortex to muscle via the corticospinal tract (Mima and Hallett, 1999; Brown, 2000; Gross *et al.*, 2000; Mima *et al.*, 2001).

In the case of the net pallidal drive to dystonic muscle shown here, it seems reasonable to view this as an overall drive of involuntary muscle activity from pallidum over 3–10 Hz. This view is supported by the core clinical observation that lesioning or high-frequency stimulation of the GP suppresses dystonic muscle activity (Krack and Vercueil, 2001; Bittar *et al.*, 2005; Vidailhet *et al.*, 2005). Also previous evidence from spectral analyses has shown that involuntary muscle spasm in primary dystonia involves a descending drive to muscle within the very same frequency band (Tijssen *et al.*, 2000, 2002; Grosse *et al.*, 2004). In line with this evidence, the amplitude of pallidal LFP activity in the 3–10 Hz band correlates with the intensity of dystonic muscle contraction over time (Chen *et al.*, 2006*a*). Microelectrode studies suggest that power and oscillatory spike triggered averages of LFP activity in this frequency band are concentrated in the internal segment of the globus pallidus, the site where functional neurosurgery seems most effective (Chen *et al.*, 2006*b*). Note that, although we confirmed focality, we made no attempt to identify the precise localization of pallidal activity coupled to dystonic EMG activity in the present study, as LFPs recorded with microelectrodes rather than stimulating deep brain (macro-) electrodes are better suited for this purpose.

Our data are compatible with a net drive from pallidum to dystonic muscle, and are in agreement with the pallidal driving deduced from spectral phase estimates in a single patient with myoclonus-dystonia, where unidirectional effects were assumed (Foncke *et al.*, 2007*a*). However, the question still remains, whether this pallidal drive is quantitatively significant in determining dystonic muscle activity. The degrees of simple coherence and directed coherence averaged over time were relatively weak. Two factors may have contributed to a comparatively weak coupling between sites. First, coupling is most likely to be indirect in the case of pallido-muscular coupling, and may become weakened at successive synaptic relays, which may also introduce non-linear dependencies between the signals which would be undetected by our linear approach. This seems likely to be a very real consideration, as connections in both afferent and efferent directions involve multiple relays. In the case of information flow from pallidum to dystonic muscle this is likely to involve input to thalamus and hence to motor cortex and/or inputs to brainstem relays to motor structures. Indeed, it may seem counter-intuitive that activity in the internal pallidum, a structure composed of inhibitory neurons projecting to the thalamus and brainstem, could lead to pathologically increased activity in the musculature. Nevertheless, the scale of simple and directed coherence was comparable to that found between cortex and muscle in healthy subjects, where coherence is thought to be largely mediated by mono-synaptic cortico-spinal pathways (Mima and Hallett, 1999; Mima *et al.*, 2001). The second factor that may have contributed to a comparatively weak coupling between sites is the averaging over time involved in simple and directed coherence estimates which would tend to underestimate drives that are not fixed over time. The time-evolving DTF was very instructive in this regard, confirming the dynamic nature of the pallidal drive to dystonic muscle, which, for short periods could account for as much as 25% of the muscle signal in the 3–10 Hz band (Fig. 3), which itself accounted for most of the power in the spectrum of the rectified EMG. This compares favourably with the degree of corticospinal coherence often reported in cortical myoclonus, a condition where exaggerated corticospinal drive to muscle causes involuntary muscle activity (Brown *et al.*, 1999; Grosse *et al.*, 2003).

Another issue that deserves further comment is the lower limit of those frequencies involved in the net pallidal drive to dystonic muscle. We elected to consider simple and directed coherence over a 3–10 Hz band so as to match our power analyses. The latter avoided frequencies under 3 Hz, in order to limit the effects of artefact from dystonic head movements. However, the directed coherence averaged over long or short-time periods suggested that there was major asymmetry of information flow even at frequencies under 3 Hz, arguing that much of such pallidal activity may have a comparable biological significance to that at higher frequencies. This is of interest in two regards. First, several studies of single neuron activity in the pallidum and thalamus suggest an excessive tendency to bursting at very low frequencies in dystonia, frequencies that may also be represented in dystonic muscle activity (Suarez *et al.*, 1997; Vitek *et al.*, 1999; Zhuang *et al.*, 2004). The power and asymmetric directed coherence between pallidal LFP and dystonic muscle over frequencies under 3 Hz therefore suggests that the bursting of single neurons may be synchronized across units, as reported over 3–10 Hz (Chen *et al.*, 2006*b*). Second, the presence of significant power, and simple and directed coherence, at very low frequencies that tends to diminish at progressively higher frequencies is compatible with a major contribution from arrhythmic but synchronized bursting in the pallidum.

Of course, this is not the exclusive pattern of synchronized activity, as some patients showed discrete peaks in their power and coherence under 10 Hz. The presence of true oscillatory synchronization in dystonia is further supported by the finding of clearly oscillatory spike triggered averages of pallidal LFPs in some patients with primary dystonia (Chen *et al.*, 2006*b*).

A final issue is to what extent the current findings apply to all dystonic features. Clinical assessment suggested that all our patients had some mobile elements to their dystonia. This may be an important point, as other authors have suggested that coherence between pallidal LFPs and dystonic EMG over the 3–10 Hz band is limited to those patients with mobile dystonia, rather than purely fixed dystonic posturing (Liu *et al.*, 2006; Foncke *et al.*, 2007*b*). Accordingly, the low frequency oscillatory drive from pallidum to muscle may possibly be absent in non-mobile dystonias.

In conclusion, the data and analyses suggest a net drive from the pallidum to dystonic neck muscles in patients with mobile primary dystonia over frequencies of $\leqslant$10 Hz. This implies that the globus pallidus is intimately involved in determining the pattern of involuntary movements in primary dystonia. We neither claim that the internal pallidum alone generates the oscillatory activity $\leqslant$10 Hz nor that pallidal neurons directly drive motor neurons. Indeed, looking for a single origin for the pathological oscillations recorded in basal ganglia disorders may be futile, given that it is likely the interaction between structures that underlies rhythmic activity (Bevan *et al.*, 2002). The novel finding here is that oscillations $\leqslant$10 Hz in muscle are partly the result of activity in a central network including the internal pallidum. A further elucidation of the precise role of the internal pallidum in the generation of 3–10 Hz oscillatory activity will require simultaneous recording at multiple points in the cortex, basal ganglia and thalamus, as well as muscle. At the present time, such opportunities in humans do not exist.

Acknowledgements

P.B. is supported by the Medical Council Research Council of Great Britain. A.S. was supported by the Bundesministerium für Bildung und Forschung (BMBF) and the EU Marie-Curie Programme as part of the Neurovers-IT project (MRTN-CT-2005-019247).

References

Astolfi L, Cincotti F, Mattia D, Babiloni C, Carducci F, Basilisco A, et al. Assessing cortical functional connectivity by linear inverse estimation and directed transfer function: simulations and application to real data. Clin Neurophysiol 2005; 116: 920–32.

Bevan MD, Magill PJ, Terman D, Bolam JP, Wilson CJ. Move to the rhythm: oscillations in the subthalamic nucleus-external globus pallidus network. Trends Neurosci 2002; 25: 525–31.

Bittar RG, Yianni J, Wang S, Liu X, Nandi D, Joint C, et al. Deep brain stimulation for generalised dystonia and spasmodic torticollis. J Clin Neurosci 2005; 12: 12–6.

Brovelli A, Ding M, Ledberg A, Chen Y, Nakamura R, Bressler SL. Beta oscillations in a large-scale sensorimotor cortical network: directional influences revealed by Granger causality. Proc Natl Acad Sci USA 2004; 101: 9849–54.

Brown P. The Piper rhythm and related activities in man. Prog Neurobiol 2000; 60: 97–108.

Brown P, Farmer SF, Halliday DM, Marsden J, Rosenberg JR. Coherent cortical and muscle discharge in cortical myoclonus. Brain 1999; 122: 461–72.

Buzsáki G, Draguhn A. Neuronal oscillations in cortical networks. Science 2004; 304: 1926–9.

Cassidy MJ, Brown P. Hidden Markov based autoregressive analysis of stationary and non-stationary electrophysiological signals for functional coupling studies. J Neurosci Methods 2002; 116: 35–53.

Cassidy MJ, Brown P. Spectral phase estimates in the setting of multidirectional coupling. J Neurosci Methods 2003; 127: 95–103.

Chen CC, Kuhn AA, Hoffmann KT, Kupsch A, Schneider GH, Trottenberg T, et al. Oscillatory pallidal local field potential activity correlates with involuntary EMG in dystonia. Neurology 2006a; 66: 418–20.

Chen CC, Kuhn AA, Trottenberg T, Kupsch A, Schneider GH, Brown P. Neuronal activity in globus pallidus interna can be synchronized to local field potential activity over 3-12 Hz in patients with dystonia. Exp Neurol 2006b; 202: 480–6.

Foncke EM, Bour LJ, Speelman JD, Koelman JHTM, Tijssen MA. Local field potentials and oscillatory activity of the internal globus pallidus in myoclonus-dystonia. Mov Disord 2007a; 22: 369–76.

Foncke EM, Bour LJ, van der Meer JN, Koelman JHTM, Tijssen MA. Abnormal low frequency drive in myoclonus-dystonia patients correlates with presence of dystonia. Mov Disord 2007b; 22: 1299–307.

Granger CWJ. Investigating causal relations by econometric models and cross-spectral methods. Econometrica 1969; 37: 424–38.

Gross J, Tass PA, Salenius S, Hari R, Freund HJ, Schnitzler A. Cortico-muscular synchronization during isometric muscle contraction in humans as revealed by magnetoencephalography. J Physiol 2000; 527: 623–31.

Grosse P, Cassidy M, Brown P. EEG-EMG, MEG-EMG and EMG-EMG frequency analysis: physiological principles and clinical applications. Clin Neurophysiol 2002; 113: 1523–31.

Grosse P, Edwards M, Tijssen MAJ, Schrag A, Lees AJ, Bhatia KP, et al. Patterns of EMG-EMG coherence in limb dystonia. Mov Disord 2004; 19: 758–69.

Grosse P, Guerrini R, Parmeggiani L, Bonanni P, Pogosyan A, Brown P. Abnormal corticomuscular and intermuscular coupling in high-frequency rhythmic myoclonus. Brain 2003; 126: 326–42.

Halliday DM, Rosenberg JR, Amjad AM, Breeze P, Conway BA, Farmer SF. A framework for the analysis of mixed time series/point process data – theory and application to the study of physiological tremor, single motor unit discharges and electromyograms. Prog Biophys Molec Biol 1995; 64: 237–78.

Kaminski MJ, Blinowska KJ. A new method of the description of the information flow in the brain structures. Biol Cybern 1991; 65: 203–10.

Korzeniewska A, Manczak M, Kaminski M, Blinowska KJ, Kasicki S. Determination of information flow direction among brain structures by a modified directed transfer function (dDTF) method. J Neurosci Methods 2003; 125: 195–207.

Krack P, Vercueil L. Review of the functional surgical treatment of dystonia. Eur J Neurol 2001; 8: 389–99.

Krauss JK, Loher TJ, Weigel R, Capelle HH, Weber S, Burgunder JM. Chronic stimulation of the globus pallidus internus for treatment of non-DYT1 generalized dystonia and choreoathetosis: 2-year follow up. J Neurosurg 2003; 98: 785–92.

Kus R, Kaminski M, Blinowska KJ. Determination of EEG activity propagation: pair-wise versus multichannel estimate. IEEE Trans Biomed Eng 2004; 51: 1501–10.

Lenz FA, Suarez JI, Metman LV, Reich SG, Karp BI, Hallett M, et al. Pallidal activity during dystonia: somatosensory reorganization and changes with severity. J Neurol Neurosurg Psychiatry 1998; 65: 767–70.

Liu X, Griffin IC, Parkin SG, Miall RC, Rowe JG, Gregory RP, et al. Involvement of the medial pallidum in focal myoclonic dystonia: a clinical and neurophysiological case study. Mov Disord 2002; 17: 346–53.

Liu X, Yianni J, Wang S, Bain PG, Stein JF, Aziz TZ. Different mechanisms may generate sustained hypertonic and rhythmic bursting muscle activity in idiopathic dystonia. Exp Neurol 2006; 198: 204–13.

Magill P, Pogosyan A, Sharott A, Csicsvari J, Boalm JP, Brown P. Changes in functional connectivity within the rat striatopallidal axis during global brain activation in vivo. J Neurosci 2006; 26: 6318–29.

Mima T, Hallett M. Corticomuscular coherence: a review. J Clin Neurophysiol 1999; 16: 501–11.

Mima T, Matsuoka T, Hallett M. Information flow from the sensorimotor cortex to muscle in humans. Clin Neurophysiol 2001; 112: 122–6.

Nolte G, Bai O, Wheaton L, Mari Z, Vorbach S, Hallett M. Identifying true brain interaction from EEG data using the imaginary part of coherency. Clin Neurophysiol 2004; 115: 2292–307.

Nunez PL. Neocortical dynamics and human EEG rhythms. New York/ Oxford: Oxford University Press; 1995.

Preacher KJ. Calculation for the chi-square test: an interactive calculation tool for chi-square tests of goodness of fit and independence [Computer software]. http://www.quantpsy.org; 2001..

Rappelsberger P, Petsche H. Probability mapping: power and coherence analyses of cognitive processes. Brain Topogr 1988; 1: 46–54.

Regan D. Human brain electrophysiology, evoked potentials and evoked magnetic fields in science and medicine. New York: Elsevier Press; 1989.

Sharott A, Magill PJ, Bolam JP, Brown P. Directional analysis of coherent oscillatory field potentials in the cerebral cortex and basal ganglia of the rat. J Physiol 2005; 562: 951–63.

Schaltenbrand G, Wahren W. Atlas for stereotaxy of the human brain. Stuttgart: Thieme; 1977.

Shen B, Nadkarni M, Zappulla RA. Spectral modulation of cortical connections measured by EEG coherence in humans. Clin Neurophysiol 1999; 110: 115–25.

Siberstein P, Kuhn AA, Kupsch A, Trottenberg T, Krauss JK, Wohrle JC, et al. Patterning of globus pallidus local field potentials differs between Parkinson's disease and dystonia. Brain 2003; 126: 2597–608.

Suarez JI, Metman LV, Reich SG, Dougherty PM, Hallett M, Lenz FA. Pallidotomy for hemiballismus: efficacy and characteristics of neuronal activity. Ann Neurol 1997; 42: 807–81.

Supp GG, Schlogl A, Fiebach CJ, Gunter TC, Vigliocco G, Pfurtscheller G, et al. Semantic memory retrieval: cortical couplings in object recognition in the N400 window. Eur J Neurosci 2005; 21: 1139–43.

Thatcher RW, Krause PJ, Hrybyk M. Cortico-cortical associations and EEG coherence: a two compartmental model. Electroencephalogr Clin Neurophysiol 1986; 64: 123–43.

Tijssen MA, Marsden JF, Brown P. Frequency analysis of EMG activity in patients with idiopathic torticolis. Brain 2000; 123: 677–86.

Tijssen MAJ, Münchau A, Marsden JF, Lees AJ, Brown P. Descending control of muscles in patients with cervical dystonia. Mov Disord 2002; 17: 493–500.

Vidailhet M, Vercueil L, Houeto JL, Krystkowiak P, Benabid AL, Cornu P, et al. Bilateral deep-brain stimulation of the globus pallidus in primary generalized dystonia. N Engl J Med 2005; 352: 459–67.

Vitek JL, Chockkan V, Zhang JY, Kaneoke Y, Evatt M, DeLong MR, et al. Neuronal activity in the basal ganglia in patients with generalized dystonia and Hemiballismus. Ann Neurol 1999; 46: 22–35.

Vitek JL, Zhang J, Evatt M, Mewes K, DeLong MR, Hashimoto T, et al. GPi pallidotomy for dystonia: clinical outcome and neuronal activity. Adv Neurol 1998; 78: 211–9.

Volkmann J, Benecke R. Deep brain stimulation for dystonia: patient selection and evaluation. Mov Disord 2002; 17 (Suppl 3): S112–5.

Wang S, Chen Y, Ding M, Feng J, Stein JF, Aziz TZ, et al. Revealing the dynamic causal interdependence between neural and muscular signals in Parkinsonian tremor. J Franklin Institute 2007; 344: 180–95.

Wang SY, Liu X, Yianni J, Aziz T, Stein J. Extracting burst and tonic components from surface electromyograms in dystonia using adaptive wavelet shrinkage. J Neurosci Methods 2004; 139: 177–84.

Zhuang P, Li Y, Hallett M. Neuronal activity in the basal ganglia and thalamus in patients with dystonia. Clin Neurophysiol 2004; 115: 2542–57.